The significance of electrochemical impedance spectra recorded during active oxygen evolution for oxide covered Ni, Co and Fe electrodes in alkaline solution

Michael E.G. Lyons, Michael P. Brandon

PII: S0022-0728(09)00115-6
DOI: 10.1016/j.jelechem.2009.03.019
Reference: JEC 12316

To appear in: *Journal of Electroanalytical Chemistry*

Received Date: 21 November 2008
Revised Date: 24 March 2009
Accepted Date: 26 March 2009

Please cite this article as: M.E.G. Lyons, M.P. Brandon, The significance of electrochemical impedance spectra recorded during active oxygen evolution for oxide covered Ni, Co and Fe electrodes in alkaline solution, *Journal of Electroanalytical Chemistry* (2009), doi: 10.1016/j.jelechem.2009.03.019

Title: The significance of electrochemical impedance spectra recorded during active oxygen evolution for oxide covered Ni, Co and Fe electrodes in alkaline solution.

Authors: Michael E.G. Lyons*, Michael P. Brandon

Affiliation and Address:

Physical and Materials Electrochemistry Laboratory,
School of Chemistry,
University of Dublin,
Trinity College,
Dublin 2,
Ireland.

*Corresponding Author. Fax: +353 1 6712826, Tel: +353 1 8962051
e-mail: melyons@tcd.ie

Abstract: Although the mechanism for the oxygen evolution reaction (OER) is likely to be similar for oxidised electrodes of the adjacent transition metals Ni, Co and Fe, the electrochemical impedance spectra, recorded for each of these anodes during oxygen evolution in 1.0 M NaOH, are significantly different in appearance. This impedance data is analysed using an approach similar to that of Cahan and Chen [1] in an earlier important article on this topic. A controversial proposal by these workers that OER "Tafel slopes" (measured by either ac or dc techniques) for many electrode systems are not in fact characteristic of the kinetics of the reaction, but instead of the potential dependent conductivity of the oxide, is dismissed on the basis of our data. In the case of Co however, it is found that the kinetics of the OER are masked by a dominant low frequency pseudo-capacitance, arising most likely from a non-homogeneous surface charge distribution associated with the oxidation of Co(III) to Co(IV) oxy-hydroxide species. A consistent interpretation of the data is provided, which envisages that Fe exhibits the most general impedance response with the spectra for the other anodes taking the form of limiting cases. Consideration is also given to the most appropriate choice of equivalent circuit model (with a firm physical basis) to aid our understanding of the complex interface at which oxygen evolution proceeds.

Keywords: oxygen evolution, impedance, Bode plot, iron electrode, cobalt electrode, nickel electrode

1. Introduction

Electrochemical impedance spectroscopy (EIS) is a potentially useful experimental tool in probing the kinetics of electrocatalytic reactions and in characterising the properties of the electrode/electrolyte interfaces at which such reactions occur. The technique has been applied extensively to the study of the anodic oxygen evolution reaction (OER) occurring on various different substrates. Amongst the anode materials for which impedance responses at overpotentials associated with significant OER current densities have been detailed are: oxidised polycrystalline Ni [2], Co [3] and Pt [4], cobalt oxides deposited on various substrates [5-7], Co and Ni mixed oxides [8,9] and alloys [10], perovskites (e.g. $La_{0.5}Ba_{0.5}CoO_3$ [11] or various ferrites[12]), IrO_2 and related materials [13-16] and various amorphous alloys[17,18].

The interpretation of EIS data is often a rather complicated task, with the most common approach involving the simulation of the interfacial system under investigation, in terms of semi-empirical electrical equivalent circuit models. Indeed such an approach has been adopted in the majority of the literature cited above and also by ourselves, where we have presented EIS measurements in tandem with dc steady state polarisation and cyclic voltammetry data, in an article on the OER at multi-cycled Fe electrodes in alkaline solution [19]. In terms of this random sample from the literature, there is reasonable agreement between the various authors regarding the general form of the appropriate equivalent circuit for the modelling of the interface between oxygen evolution anodes and aqueous electrolyte solutions. Most workers comment briefly on the significance of the various elements of their envisaged equivalent circuit, before detailing the optimised values of these elements obtained by complex non-linear least squares (CNLS) fitting of the raw impedance data (for a given overpotential η) to that model. A more thorough discussion of the form of the equivalent circuit model relevant to the study of oxygen evolution on oxide electrodes was presented some time ago by Cahan and Chen [1]. These authors reached conclusions that challenge the conventional wisdom regarding the significance of EIS data recorded during oxygen evolution. In view of this, they proposed an equivalent circuit model, which although containing essentially the same elements as the conventional model, envisages a different connection scheme. In the present article, we subject OER impedance data that we have recorded for passive oxide covered Ni, Co and Fe electrodes, to an analysis similar to that of Cahan and

Chen, in order to establish whether their alternative equivalent circuit model (with its associated and rather profound implications) is applicable or if the conventional model is more appropriate. Here we focus largely on physical models of oxygen evolution anodes – readers who seek more detailed information on our electrode systems, with regard to aspects such as the mechanism of the OER or the nature of the catalytic oxide phases, are referred to complementary articles [19,20].

2. Experimental

The electrodes were prepared from the following "as supplied" polycrystalline samples of the relevant metals: Ni – 1 mm thick foil, Alfa Aesar (Johnson Matthey), purity 99.9945%, Co – 2 mm diameter wire, Aldrich, purity 99.9+%, "fresh" Fe – 1 mm thick foil, Alfa Aesar, purity 99.995% and "aged" Fe – 2mm diameter wire, Aldrich, purity 99.9+%. Sections of the foils (exposed geometric surface area = 0.16 cm^2) were sealed horizontally across the bottom of glass tubes using epoxy (Araldite). Connectivity to the external circuit was provided by attaching copper wire to the reverse of the foil using conductive epoxy. Electrodes were prepared from the wire samples simply by sealing lengths of the wire into glass tubes with the cross sectional area (~0.0314 cm^2) exposed at one end. In the course of the text various pre-treatment regimes will be outlined – it is worth commenting however, that prior to each experiment, all electrodes were polished to a mirror "bright" finish using a slurry of 0.05 micron alumina powder.

Solutions of NaOH (1.0 M) were used as electrolytes. These were prepared from NaOH pellets (BDH AnalaR®, minimum 98% purity) using millipore water (resistivity 18.1 MΩ cm). A conventional, un-thermostatted, three electrode cell arrangement was adopted. A platinum wire electrode (CH Instruments, Inc. -catalogue no. CHI 115) was employed as the counter electrode, while the reference electrode was a mercury-mercuric oxide (Hg/HgO, 1 M NaOH) electrode as supplied by Radiometer Analytical (cat no. XR400). All electrochemical measurements were performed using a PC controlled Zahner IM6 system. In recording steady state polarisation characteristics, a "staircase" type, dc potential-time regime was applied in the direction of increasing potential. With a step height of 5 mV, a step width of 120 secs. was found to be adequate for the achievement of a steady current for all systems. The impedance spectra were measured separately by employing a 10 mV p-p amplitude, sine wave potential perturbation on the dc potential. The dc potential was

changed step wise in the positive direction, with sufficiently long delays to achieve steady state conditions. This has been checked by applying Kramers-Kronig tests to the measured spectra. All measured quantities are quoted with respect to the geometric area of the relevant electrode. The CNLS fitting was performed using the SIM software of the IM6 system.

3. The Cahan and Chen analysis

3.1 The ideal general form of the Bode plot during oxygen evolution and equivalent circuits

As indicated in the Introduction, the main focus of the present article is to analyse our OER impedance spectra using principles outlined by Cahan and Chen in a discussion of EIS data recorded during oxygen evolution for a passive oxide covered Fe electrode in borate buffer solution (pH 8.4) and also for an oxide covered Au anode in 1 N $HClO_4$ [1]. These workers produced a schematic of the Bode plot that would arise for the OER occurring at the surface of an oxide electrode in the idealised case where the capacitive processes behave as ideal capacitors and the characteristic time constants for the various relaxation processes differ significantly. We have constructed a similar plot in Fig. 1, although we use different notation and also include the idealised form of the phase angle vs. log frequency characteristic. Such a Bode plot might be modelled by either of the circuits in Fig. 2 – however before explaining our preference for Circuit A, we consider the significance of each circuit element and its associated section of the Bode plot. The following discussion has been informed by the observations of Harrington and Conway [21] on the equivalent circuits most commonly proposed for the modelling of EIS data obtained for faradaic reactions involving electrosorbed intermediates.

The high frequency resistive response, R_Ω, represents the uncompensated solution resistance, C_{film} and R_{film} are respectively related to the dielectric properties and the resistivity of the oxide film, while C_{dl} models the double layer capacitance. The resistive elements R_p and R_s are connected to the kinetics of the interfacial charge transfer reaction. Harrington and Conway have rejected a common interpretation that R_p and R_s are the charge transfer resistances of the electrosorption and desorption processes respectively, asserting that these elements are the properties of two or more steps in the overall reaction. Finally, $C_ø$ is the value of a capacitance, which in parallel

with R_s in an equivalent circuit model, correctly models the relaxation of the charge associated with the adsorbed intermediate.

Cahan and Chen [1] commented that $C_{ø}$ is normally >> C_{dl}, and that for an oxide film thicker than a few angstroms with any reasonable value of dielectric constant, C_{film} < C_{dl}. Scenario 1 in the schematic log|Z| vs. log frequency Bode plot of Fig. 1, then represents the situation where $R_{Ω}$ << R_{film} << R_p. With regard to this plot it should be noted that although we have identified particular flat (slope = 0) regions with a given resistive element, the total resistance at any of these regions is actually the sum of the indicated resistance and all of the resistances that are sensitive to detection at higher frequencies. For example the total resistance over the region labelled R_p is actually R_p + R_{film} + $R_{Ω}$, since these elements are added in series in the circuit models of Fig. 2. However, since R_p >> R_{film} >> $R_{Ω}$, it is R_p that is the dominant contribution to the aforementioned resistive section of the Bode plot and so for clarity in the discussion that follows it is appropriate, to a good approximation, to attribute that region of the plot to the impedance response of R_p. This also implies that the overall resistance, R_{lf}, at the low frequency limit of the experiment is approximately equal to the *total Faradaic resistance*, R_{far}, where R_{far} = R_p + R_s. Similar comments apply to the diagonal (slope = -1) regions of the idealised plot, which we have labelled in terms of the dominant capacitive contribution over the relevant frequency range. Circuits A and B of Fig. 2 feature a capacitive element in series with a parallel combination of two other capacitive components. Since parallel capacitances add directly, but serial capacitances add reciprocally, it is clear that the mathematical significance of the capacitive contribution in the C_{dl} and $C_{ø}$ regions isn't as simple as was discussed for the resistive case, and in fact differs depending on whether we admit Circuit A or B.

It is worth noting at this point, that for a given overpotential, η, if the values of R_{far} and the OER steady state current density, i, are known, the instantaneous value of the Tafel slope, b, can be ascertained through the expression:

$$b = 2.303 i R_{far} \qquad (1)$$

In the case of the ideal OER impedance spectrum of Fig. 1, scenario 1, where $R_{far} \approx R_{lf}$, it is therefore permissible to write (to a good approximation) that:

$$b = 2.303 i R_{lf} \qquad (2)$$

3.2. More specific cases and comparison with experiment

Taking the discussion a step further, Cahan and Chen commented that in the case where $R_{film} << R_{\Omega}$, the R_{film} line segment moves down until the C_{film} section of the plot disappears. Therefore R_{film} and C_{film} are no longer experimentally accessible, as in scenario 2 of Fig 1. This is an example of a general phenomenon, which they have highlighted, whereby the removal of a series resistive and/or capacitive element from an appropriate equivalent circuit model, causes the log|Z| vs. log frequency plot (or part thereof) of Fig. 1 to move downward and to the left. The converse will clearly be true for the interposition of any resistive or capacitive element in series with the network.

On the other hand at potentials where $C_{ø}$ is no longer significant, scenario 1 of Fig 1 will alter to scenario 3. This is equivalent to removing the $C_{ø}$ component from Circuit A or B. So the removal of a parallel resistive and/or capacitive element has the effect of translating the curve (or a part thereof) upward and to the right.

Examining the Bode plots they obtained at various potentials during oxygen evolution for the passive film on iron in borate buffer solution (pH 8.4), Cahan and Chen [1] concluded that their results were best explained by scenario 4 of Fig. 1 – i.e. where $R_{film}>>R_s$. At a potential of 1.1 V (vs. R.H.E.), which is below that associated with significant oxygen evolution currents, the Bode representation of their data (frequency range of $10^{-1} \rightarrow 10^{4}$ Hz) was characterised by a diagonal line with no resistive plateau at the low frequency end. In other publications [22,23] the same authors had shown that the passive film in this region of potential was an insulator with a resistivity of ~ 10^{15} Ω cm. They thus proposed that the Bode plot at this potential, arose due to the situation where $R_{film}>>R_s$, but with no low frequency resistive shelf being observed, since in this case R_{film} is so high that the associated time constant, τ_{film} ($=R_{film}C_{film}$), would only be fully characterised on a longer time scale than that of the experiment – i.e. at frequencies below 10^{-1} Hz.

As the potential was increased into the range associated with oxygen evolution, Cahan and Chen noted that the experimental log|Z| vs. log freq. curve moved downwards, a situation that they interpreted in terms of Circuit B (Fig. 2), as being due to a new RC circuit (the $R_sC_{ø}$ loop) appearing in parallel with the $R_{film}C_{film}$ loop. At a potential of 1.5 V the authors observed the appearance of a low frequency resistive plateau – they postulated that this was largely due to R_{film} on the basis that, at this potential the value

of the film resistance is ca. 10^5 Ω, and therefore is just resolvable by an impedance measurement at 10^{-1} Hz. With further increase of the applied potential, the low frequency resistance decreased in such a manner that would yield an effective "Tafel slope" of 50 – 60 mV dec^{-1} according to eqn. (2).

These observations led Cahan and Chen to arguably the most controversial assertion ever contained in a publication on the OER – namely that, for the particular system under study, the "Tafel slope" as measured, either directly by the steady state polarisation method, or extracted from EIS measurements, was due, not to the kinetics of the OER but to the increasing conductivity of the passive film over a range of potentials anodic to ~ 1.5 V. This was envisaged to arise, because, for scenario 4 of Fig. 1, R_{lf} is dominated by R_{film} and does not characterise the kinetically significant R_{far} at all. The overall dc current density at a given overpotential will then be governed by the resistivity of the oxide, implying that the actual kinetics of the OER may actually be much faster than those characterised by the apparent "Tafel slope". The authors explained this phenomenon in terms of what they called the "chemi-conductor" model, the principles of which were outlined in a separate publication [24]. The scenarios of Fig. 1, along with the significance of R_{lf} in each case are summarised in Table 1.

Cahan and Chen [1] conducted further EIS studies on an Au electrode in 1 N $HClO_4$ solution, and again reached the conclusion that a poorly conducting oxide film masked the true OER kinetics. On the basis of their two sample systems they made the following rather bold statement [24] that "the previous literature which measures the apparent kinetics of oxygen evolution, may simply have been measuring the dc resistivity of the film rather than the kinetics".

Although the foregoing assertion laid down the gauntlet for future workers to prove that experiments purporting to measure the kinetics of the OER, actually do so, this is a challenge that, to the best of our knowledge, has not been taken up. From our point of view, this question is inseparable from the issue of choosing the appropriate equivalent circuit model for our EIS data – can we adopt Circuit A or are we forced to admit Circuit B, thereby conceding that our steady state polarisation and EIS data [19,20] is effectively worthless with regard to the study of the kinetics of the OER.

4. Results and discussion

4.1. The OER on passive oxide covered iron electrodes

Perhaps the most appropriate starting point for the analysis of our data lies with oxidised Fe electrodes, since, not only was this was the metal studied by Cahan and Chen [1], but these also display the most general EIS behaviour during oxygen evolution.

EIS spectra recorded at various potentials for a pre-reduced Fe electrode in 1.0 M NaOH, are presented in Fig. 3. Also included, as an inset, is a dc steady state polarisation plot for the same system. In this article, for each set of impedance spectra, the complementary dc polarisation curve is provided for reference purposes. We have discussed these Tafel plots in detail elsewhere and in each case a reference is provided for the interested reader. Before conducting either the dc or impedance measurements, the Fe electrode was polarised in 1.0 M NaOH solution at a cathodic potential of –1.1 V for a period of 5 minutes before being subjected to one potentiodynamic cycle between the limits of –1.175 and 0.625 V at a scan rate of 40 mV s^{-1}.

Examining the phase angle vs. log freq. curves, it is obvious that the most rapid relaxation process occurs at frequencies in the vicinity of 10^4 Hz. It will be shown later that for oxidised Ni and Co electrodes, no relaxation process is detected on such a short timescale. It would thus seem unlikely that the aforementioned relaxation process is associated with the double-layer capacitance, since it is difficult to understand why this would discharge much more rapidly in the case of Fe, than for Ni or Co. Consulting the literature, reveals that while Castro et al. [6] observed just one pseudo-semi-circle in the Nyquist representation of OER impedance data for Co oxide electrodeposited on Ni and Pt disk electrodes, they noted an additional capacitive contribution in the high frequency range for the same oxide deposited on an Fe substrate. Kessler et al. [17] used EIS to study the OER at the amorphous alloys G14 ($Fe_{60}Co_{20}Si_{10}B_{10}$) and G16 ($Co_{50}Ni_{25}Si_{15}B_{10}$) in 1.0 M KOH. In the case of the predominantly iron alloy (G14) two capacitive semi-circles were noted in the complex plane presentation of the results. For the G16 electrode the higher frequency feature was apparently absent. In both of the aforementioned cases the authors attributed the high frequency semi-circle to the dielectric properties of the anodic oxide layer. It would therefore seem that impedance measurements on Fe (or Fe based) anodes are sensitive to an oxide film capacitance, that is not detected for Co, Ni or Pt electrodes. This behaviour is not restricted to just Fe – for example similar high frequency impedance features have been noted by Conway and Liu [5] studying the OER at

Co_3O_4 deposited on a Ti substrate, and by Da Silva et al. [15] for Ti-supported (Ru + Ti + Ce) O_2 electrodes. In the latter case the authors have proposed that a highly resistive TiO_2 anodic oxide film (TiO_2 interlayer) that forms between the metallic Ti support and the conductive oxide material during electrode preparation, acts as a dielectric material, giving rise to the high frequency capacitive response.

Returning to Fig. 3, a comparison of the log|Z| vs. log freq. curve for the "double-layer" region (E = -1.1V) with that recorded at 0.6 V, allows several inferences to be made. Referring to the dc OER steady state polarisation curve, it is evident that 0.6 V is slightly below the potential at which significant OER currents arise, while voltammetry indicates that this potential is not apparently associated with any other faradaic process [19]. The curve for 0.6 V is translated upward and to the right relative to that for –1.1 V. Following the logic of Cahan and Chen [1] this is indicative of the addition of a series capacitive and/or resistive element to the equivalent circuit model applicable in the double layer region. Assuming that the impedance response in the double layer region can be modelled in terms of a R_pC_{dl} loop in series with R_Ω, the "upward" translation of the log|Z| vs. log freq. curve, is readily understood by the serial addition of a $R_{film}C_{film}$ loop arising from the development of the passive film between –1.1 V and 0.6 V.

There is an obvious change in the form of the log|Z| vs. log freq. curve as the potential is raised above 0.6 V into the region which is characterised in the steady state log$i$ vs. E curve by a Tafel slope of b = 45 mV dec^{-1}. The capacitive response of the film at frequencies → 10^4 Hz remains essentially constant, however an inflection appears in the curves at frequencies immediately below this range. This arrest region covers frequencies from approximately 10^3 Hz up to those at which the film capacitance becomes manifest. As the potential is increased, this shelf region becomes more obvious as it moves downward – simultaneous to this the phase angle maximum corresponding to the relaxation of the film capacitance is shifted towards higher frequencies. The later observation is consistent with a decrease in R_{film} with potential since, as previously noted C_{film} remains largely constant. It is therefore appropriate to associate R_{film} with the aforementioned downward moving shelf region. Thus we reach the important conclusion, that for this Fe electrode in 1.0 M NaOH, the low frequency impedance response at potentials corresponding to the Tafel region of the OER steady state polarisation curve, is *not* dictated primarily by the resistivity of the anodic oxide film. Therefore we can be confident that the Tafel slope extracted from

this impedance data via eqn. (2), or indeed as measured by dc steady state polarisation methods, is in fact characteristic of the kinetics of the OER. Furthermore, the above discussion implies that the appropriate equivalent circuit model for this system is Circuit A (Fig. 2).

One might question why the log|Z| vs. log freq. curves of Fig. 3 do not display distinct diagonal regions corresponding to the impedance responses of the double layer capacitance and the adsorption pseudo-capacitance, or a horizontal (or at least low slope) region corresponding to the resistive element R_p, as envisaged in scenario 1 of Fig. 1. The primary reason for this is the poor separation of the time constants related to the relaxation of the double layer and the coverage of the OER intermediate species. Furthermore, caution is required with the results of the CNLS fitting to an equivalent circuit, of impedance data characteristic of two relaxation processes having poorly separated time constants, as was discussed by Macdonald et al. [25]. Bearing this in mind, CNLS fitting of the raw data of Fig. 3 to Circuit A was performed. The optimum fit parameters are included as supplementary data.

4.2. Aged iron electrodes

Any lingering scepticism, regarding the need for a three *RC* loop equivalent circuit for the simulation of the impedance response of passive oxide covered Fe electrodes at lower oxygen evolution overpotentials in alkaline solution, should be dispelled by the EIS data presented in Fig. 4. This data was recorded for an "aged" Fe electrode, which was pre-reduced at E = -1.3 V for 15 minutes in 1.0 M NaOH and then subjected to a single potentiodynamic cycle in the same solution (lower limit and starting potential: –1.175 V, upper limit: 0.625 V, sweep rate 40 mV s^{-1}) before the acquisition of the spectra of Fig. 4. Here an "aged" electrode refers to one used in many (> 40 over the course of four months) OER polarisation experiments, and, as we discuss elsewhere [19] these anodes are possessed of rougher, more dispersed and hydrated catalytic oxide surfaces, relative to fresher iron electrodes such as that characterised in Fig 3. Referring to the phase angle vs. log freq. curves for E = 0.7 or 0.72 V, three capacitive maxima are obvious as is envisaged in scenario 1 of Fig. 1. Again the observation of distinct regions of the impedance spectra corresponding to C_{film}, R_{film}, $C_{ø}$, R_s etc. confirms that the low frequency resistance will be dominated by the faradaic resistance and that measured Tafel slopes [19] will be characteristic of the kinetics of the OER.

It is evident that the low frequency phase angle maximum becomes less significant as the potential is increased and is effectively absent for the data recorded at E = 0.76 and 0.8 V. This is an experimental manifestation of scenario 3 of Fig. 1, which is the limiting form of scenario 1 when the potential moves outside the range over which $C_{ø}$ is significant. The above observation and conclusion is consistent with our detailed discussion of the kinetics of the OER at "aged" Fe electrodes [19], in which it is envisaged that for higher potentials (including 0.76 and 0.8 V) the reaction is proceeding under adsorption conditions where the total fractional coverage, θ, of the intermediate species approachs unity (i.e. $\theta \rightarrow 1$). Intuitively, we expect $d\theta/dE$, and hence the adsorption pseudo-capacitance, to be insignificantly small in this region of potential. This is supported by the results of CNLS fitting to Circuit A, which are again included as supplementary data.

The closest observed approach of an experimental spectrum to scenario 1 of Fig. 1, is that recorded for the aged Fe electrode at E = 0.72 V (Fig. 4). Clearly there is still quite a discrepancy between even this data and the ideal log|Z| vs. log freq. plot with its horizontal resistive sections and diagonal capacitive regions. In addition to the temporal overlap of relaxation processes, frequency dispersion in the capacitive responses contributes to the observed "non-ideality". While the capacitance of an ideal parallel plate capacitor is independent of the frequency of the current in an ac circuit (hence the diagonal slope of –1 for the capacitive sections in Fig 1.), for real electrochemical interfaces it is generally observed that the various "capacitive" components exhibit some frequency dependence. In a Bode plot, this is manifested by a decrease in the magnitude of the slope of the log|Z| vs. log freq. trace (from |-1|) over the range of frequencies at which the capacitive process in question dominates the overall impedance response. For the double layer capacitance, it is generally agreed that it is surface roughness and inhomogeneity that leads to the deviation from ideal behaviour, although the mechanism by which the surface non-uniformity precipitates frequency dispersion is still somewhat controversial [26,27].

In order to treat frequency dispersion, we have admitted *constant phase elements* (CPEs) in place of pure capacitive components in the equivalent circuit models of Fig. 2. CPEs deal with the deviation from ideal capacitive behaviour, in an empirical manner, by expressing the impedance Z_{CPE} of a capacitive process displaying frequency dispersion as:

$$Z_{CPE} = A(j\omega)^{-\alpha} \qquad (3)$$

In eqn. (3), $A = 1/C_{\alpha=1}$, where $C_{\alpha=1}$ is the value of the capacitance in the absence of frequency dispersion, and α is an exponent ($\alpha \leq 1$ for a physically reasonable situation) equal to unity in the case of an ideal capacitor. When required to fit data to a CPE, the SIM fitting program returns values for $C_{\alpha=1}$ and α. Accordingly, this format is adopted for all fitted capacitance values quoted in this article and its supplementary data. Pajkossy [27] has commented that it can generally be taken as a rule of thumb that, the rougher an electrode surface, the larger the deviation from ideal capacitive impedance, and it therefore follows, the smaller the value of the CPE α parameter yielding by CNLS fitting of the data.

It is instructive to compare the optimum fitting parameters calculated for the fresh pre-reduced iron electrode at E = 0.71 V to those obtained for the aged iron anode at E = 0.72 V – see Table 2. It is noteworthy, that for both systems, it is the high frequency oxide film CPE, C_{film}, that displays the "most ideal" capacitive behaviour (i.e. α parameter closest to unity). This observation may be consistent with the concept [15] (outlined in sec. 4.1), of a resistive oxide interlayer acting as a dielectric between the metallic electrode and a more conductive outer oxide region – such an arrangement might be expected to behave in a significantly similar manner to a hardware parallel plate capacitor. As previously mentioned it is envisaged that the aged electrode of Fig. 4 has a significantly rougher outer oxide surface than the fresher specimen of Fig. 3 – in fact using the OH_{ads} desorption technique of Ho and Piron [28] we have found that the roughness factor of the former is approximately twice that of the latter [20]. This observation is bourne out by the values of the double layer CPE, $C_{dl\ \alpha=1}$, parameters of Table 2, with significantly less frequency dispersion in the case of the fresher electrode (α = 0.85) compared to the aged anode (α = 0.74).

4.3. Passive oxide covered cobalt electrodes

Impedance data recorded for a polycrystalline Co electrode in 1.0 M NaOH at various potentials are presented in Bode format in Fig. 5. Prior to the EIS measurements, the

electrode was pre-reduced (also in 1 M NaOH) at E = –1.15 V for 5 minutes, then cycled at 40 mV s^{-1} between –1.22 and 0.6 V (anodic direction first).

In the cases of the Fe data of Figs. 3 and 4, the oxide film electrical properties dominate the impedance response at frequencies in the approximate range of 5 – 50 KHz. By contrast, the higher frequency maxima in the phase angle vs. log freq. plots of Fig. 5 appear at lower frequencies – between 10^2 and 10^3 Hz. This is the same frequency range that we associated with the impedance response of the double layer capacitance for the Fe electrodes. It would therefore seem that for the oxidised Co electrode, the shorter time constant relaxation process is associated, not with the electrical properties of the anodic oxide film, but rather with the double-layer capacitance.

Indeed, the potential variation of the impedance response in this frequency range conforms to the expectations for the double layer capacitance. Consider the relatively steep region, between approximately 10^2 and 10^3 Hz, of the log|Z| vs. log freq. curves of Fig. 5. Cyclic voltammograms presented elsewhere [20] indicate that at E = 0.35 V for Co electrodes in 1.0 M NaOH, the principal faradaic process involves the formation of the outer hydrous region of the passive oxide film by the oxidation of Co(II) species to Co(III) based oxy-hydroxide entities. On the other hand, potentials from 0.55 V upwards are associated with significant oxygen evolution current densities. The decrease in |Z| between 0.35 V and 0.55 V can then be rationalised in terms of an increase in the double layer capacitance (recall that $C \propto 1/|Z|$) associated with either increasing surface roughness as the passive film is further oxidised, or a change in the nature of the double layer due to OH^- ion adsorption at high anodic potentials (as was proposed by Bockris and Otagawa [29] for a $Nd_{0.9}Sr_{0.1}CoO_3$ electrode also in 1.0 M NaOH), or indeed to a combination of these factors.

For the lower oxygen evolution current densities associated with the potentials between 0.55 and 0.64 V, |Z| remains essentially constant over this range of frequencies – however for the higher OER current density associated with E = 0.74 V, the capacitance decreases, as evidenced by an increase in |Z|. As proposed by Da Silva et al. [13], who noted similar behaviour with IrO_2 electrodes, the effect is most likely caused by vigorous oxygen bubble formation at higher OER overpotentials. The double layer capacitance is proportional to the extent of the electrode surface area in physical contact with the electrolyte solution. This “wettable” area may be diminished

by the momentary adhesion of gas bubbles to the oxide surface, or by the temporary exclusion of some of the "inner" surface area associated with pores and fissures in the oxide surface, as these regions become occupied by gaseous oxygen.

If the shorter relaxation process is indeed related to the double layer capacitance, then these spectra are manifestations of scenario 2 of Fig. 1 – i.e. $R_{film} << R_{\Omega}$ and so C_{film} becomes experimentally inaccessible. Furthermore, the obvious presence in Fig. 5 of distinct regions dominated by C_{dl}, R_p and $C_{ø}$ indicates that for oxidised Co electrodes in 1.0 M NaOH, as with oxidised Fe anodes, the kinetics of the OER are *not* masked by the electrical behaviour of a poorly conducting oxide film.

Again the optimised values for the CNLS fitting of the data of Fig. 5 to Circuit A are included as supplementary data. Perusal of this data highlights large errors in the fitted values of R_s. Examining Fig. 5, we note the absence, for lower overpotentials, of the low frequency, R_s dominated, resistive plateau, envisaged in scenario 1 of Fig. 1. Accordingly, phase angles with a large magnitude of 60-75º, indicative of capacitive domination of the impedance response, are noted at 0.1 Hz for values of $E < 0.64$ V. These observations reveal that R_{far} (recall sec. 3.1) is not characterised for lower overpotentials at the low frequency limit.

This contrasting behaviour in the EIS responses of the iron and cobalt anodes with respect to the low frequency resistance, suggests that the *RC* time constant, τ_{lf}, of the relevant relaxation process is relatively longer in the case of the latter electrode. It is evident from the accompanying steady state polarisation plots, that the lower OER Tafel regions for both the fresh Fe electrode of Fig. 3 and the Co electrode of Fig. 5 extend for ca. 2.5 decades in log i from ~ 10^{-5} A cm^{-2} upwards, with $b \approx 45$ mV dec^{-1}. This implies that for each of the systems, similar values of R_{far} (and thus R_s) prevail across the lower Tafel regions. Therefore the higher *RC* product in the case of the Co anode must arise from a larger pseudo-capacitive contribution in comparison with the Fe electrode. This suggestion is supported by the relative magnitudes of the optimised $C_{ø}$ values, obtained for each of the systems by CNLS fitting (see supplementary data).

A survey of the literature reveals that capacitive dominance of the low frequency impedance response is often observed (though rarely remarked upon) during oxygen evolution in 1.0 M OH^- solutions for electrodes of cobalt oxides. For example, the EIS data of Wu et al. [8], shows that R_{far} is well resolved at low frequencies for electrodes consisting of Co+Ni mixed oxide phases, but not for an entirely Co based oxide. Likewise, impedance spectra presented by Kessler and co-workers [17] indicate that

while R_{far} is clearly resolved at 10^{-1} Hz for an electrode of the $Fe_{60}Co_{20}Si_{10}B_{10}$ alloy, the same is not true, even at 10^{-3} Hz, for the $Co_{50}Ni_{25}Si_{15}B_{10}$ alloy, with its larger Co content. Dominant capacitive responses at the low frequency limit of EIS spectra have also been reported at lower OER overpotentials for anodes constructed from electrodeposited cobalt oxides [6] and the $Ni_{50}Co_{25}P_{15}B_{10}$ alloy [18]. The most likely explanation for this phenomenon is that the low frequency capacitive response is dominated by an additional pseudo-capacitive contribution in parallel to that arising from the potential dependent coverage of OER intermediate species. Specifically, it has been proposed [6,18] that the "additional" pseudo-capacitance arises from a non-homogeneous charge distribution associated with the surface oxidation of Co(III) to Co(IV) species.

As a direct result of the large low frequency pseudo-capacitance the kinetically significant R_{far} is inaccessible on a practically useful experimental timescale in the case of oxidised Co electrodes in 1.0 M OH^- solution. This is therefore, an example of the kinetics of oxygen evolution being masked by a different physicochemical process – not the potential dependent electrical resistance of the oxide film as envisaged by Cahan and Chen[1], but rather the potential dependence of an inhomogeneous charge distribution associated with the further oxidation of the surface of that film.

4.4. Passive oxide covered nickel electrodes

Impedance spectra are presented in Fig. 6 for a passive oxide covered polycrystalline nickel electrode in 1.0 M NaOH. Pre-treatment involved the polarisation of the electrode at 0 V for a period of 5 minutes in 1.0 M NaOH, subsequent to which the electrode potential was swept once from –0.5 V to 0.675 V and back, at 40 mVs^{-1}. Cyclic voltammograms [20] indicate that increasing the potential beyond ~ 0.43 V sees the onset of the further oxidation of the Ni(II) based passive oxide to a non-stoichiometric Ni(III)/Ni(IV) based oxy-hydroxide phase, in what is a widely studied solid-state electrochemical reaction [30]. The included steady state polarisation data suggests (for the pre-treatment outlined above) that oxygen evolution is the predominant faradaic process for E > 0.55 V, with a lower Tafel region of slope b = 40 mV dec^{-1} extending to ~ 0.63 V.

On initial inspection the EIS data recorded within the aforementioned Tafel region seem to conform to scenario 4 of Fig. 1, with the log|Z| vs. log freq. plots apparently displaying only one section of constant negative slope, between two flat shelf sections

at the high and low frequency extremes. As with the iron electrodes, further insight may be gained by examining EIS data for a more aged nickel anode exhibiting a greater degree of surface roughness – see Fig. 7. It should be noted in this case, that the electrode was not subject to pre-treatment beyond polishing and displayed somewhat superior catalytic activity relative to the anode of Fig. 6, with the ca. 40 mV dec^{-1} Tafel region being observed between ~ 0.52 and 0.6 V. While the log|Z| vs. log freq. plots of Fig 7. are similar in form to those of Fig. 6, the significant observation is the presence of two maxima in the phase angle characteristics for lower overpotentials (i.e. 0.56 and 0.58 V). The phase angle maximum for the shorter relaxation process arises at a frequency in the range of 10^2 – 10^3 Hz, which by comparison with the analyses of secs. 4.2 and 4.3, is consistent with the response of the double layer capacitance. We therefore propose that, just as for the Co data of Fig. 5, the Ni spectra of Figs. 6 and 7 are manifestations of the situation depicted by scenario 2 of Fig. 1, Thus we conclude that the spectra of Fig. 6 are not due to a single $R_{film}C_{film}$ relaxation process (scenario 4) but rather to a superposition of the R_pC_{dl} and $R_sC_{ø}$ relaxation processes. Circuit A is therefore the appropriate model for the simulation of the data of Figs. 6 and 7 – the "best fit" values of the circuit elements are available as supplementary data. Note that we don't claim that the conclusions of Cahan and Chen [1,24] are incorrect for the systems that they studied (Fe in borate buffer solution (pH 8.4) and Au in 1 N $HClO_4$), however we have shown that they are not more generally true. Indeed, one of the present authors [32] has shown that the passive films formed on Fe at pH 8.5 and at pH 14 are significantly different in nature.

5. Conclusions

Despite the fact that the OER proceeds via similar mechanisms [19,20] for oxidised nickel, cobalt and iron electrodes in 1.0 M NaOH, the impedance responses are visually quite different with distinctive features arising for each system. EIS data for potentials corresponding to the lower Tafel region in complimentary dc steady state measurements, have been shown to be characteristic of at least two relaxation processes. This renders inapplicable to our electrode systems the controversial proposal of Cahan and Chen [1], that the impedance response for many oxygen evolution anodes characterises just a single relaxation process related to the conductivity (R_{film}) and dielectric properties (C_{film}) of the oxide film. At a fundamental

level this means that either dc polarisation or ac impedance measurements conducted on our electrodes during oxygen evolution are characteristic of the kinetics of the OER (although see comment below for Co) and not of the conductivity of the passive oxide. The two ubiquitous relaxation processes are related to the double layer capacitance (R_pC_{dl} time constant), and on a longer timescale, the charge associated with the intermediate species that partake in the OER ($R_sC_{ø}$ time constant).

In the case of Co anodes, an additional low frequency pseudo-capacitance is present in parallel with the aforementioned $C_{ø}$. This means that the kinetically significant, total faradaic resistance, R_{far}, is not resolved on a useful timescale, and thus EIS is not useful in probing the kinetics of the OER for Co electrodes in 1.0 M OH^- solutions. Impedance measurements are sensitive to an additional high frequency relaxation process in the case of oxidised Fe anodes. This can be identified with the $R_{film}C_{film}$ response – however R_{film} is of a relatively low magnitude and thus the kinetics of oxygen evolution are not masked, as was envisaged by Cahan and Chen. On the basis of our analyses of the three electrode systems, it has been concluded that Circuit A of Fig. 2 is in general the most appropriate equivalent circuit model for the simulation of electrode/electrolyte interfaces during oxygen evolution.

References

[1] B.D. Cahan, C.T. Chen, J. Electrochem. Soc. 129 (1982) 700-705.

[2] M. Cappadonia, J. Divisek, T. von der Heyden, U Stimming, Electrochim Acta. 39 (1994) 1559-1564.

[3] H. Willems, A.G.C. Kobussen, J.H.W. De Wit, G.H.J. Broers, J. Electroanal. Chem 170 (1984) 227-242.

[4] B.E. Conway, T.-C. Liu, Langmuir 6 (1990) 268-276.

[5] B.E. Conway, T.-C. Liu, Ber. Bunsen-Ges. Phys. Chem. 91 (1987) 461-469.

[6] E.B. Castro, C.A. Gervasi, J.R. Vilche, J. Appl. Electrochem. 28 (1998) 835-841.

[7] S. Palmas, F. Ferrara, A. Vacca, M. Mascia, A.M. Polcaro, Electrochim. Acta. 53 (2007) 400-406.

[8] G. Wu, N. Li, D-R. Zhou, K. Mitsuo, B-Q. Xu, J. Solid State Chem. 177 (2004) 3682-3692.

[9] E.B. Castro, S.G. Real, L.F. Pinheiro Dick, Int. J. Hydrogen Energy. 29 (2004) 255-261.

[10] B. Chi, J. Li, X. Yang, Y. Gong, N. Wang, Int. J. Hydrogen Energy. 30 (2005) 29-34.

[11] A.G.C. Kobussen, J. Electroanal. Chem. 126 (1981) 199-220.

[12] R.N. Singh, N.K. Singh, J.P. Singh, Electrochim. Acta 47 (2002) 3873-3879.

[13] L.A. Da Silva, V.A. Alves, M.A.P. Da Silva, S. Trasatti, Electrochim. Acta 42 (1997) 271-281.

[14] V.A. Alves, L.A. Da Silva and J.F.C. Boodts, Electrochim. Acta 44 (1998) 1525-1534.

[15] L.M. Da Silva, K.C. Fernandes, L.A. Faria, J.F.C. Boodts, Electrochim Acta 49 (2004) 4893-4906.

[16] J-M. Hu, J-Q. Zhang, C-N. Cao, Int. J. Hydrogen Energy 29 (2004) 791-797.

[17] T. Kessler, J.R. Vilche, M. Ebert, K. Jüttner, W.J. Lorenz, Chem. Eng. Technol. 14 (1991) 263-269.

[18] K.K. Lian, D.W. Kirk, S.J. Thorpe, J. Electrochem. Soc. 142 (1995) 3704-3712.

[19] M.E.G. Lyons, M.P. Brandon, Phys. Chem. Chem. Phys. 11 (2009) 2203-2217.

[20] M.E.G. Lyons, M.P. Brandon, J. Electroanal. Chem. submitted for publication.

[21] D.A. Harrington, B.E. Conway, Electrochim. Acta. 32 (1987) 1703-1712.

[22] B.D. Cahan, C.T. Chen, J. Electrochem. Soc. 129 (1982) 17-26.

[23] B.D. Cahan, C.T. Chen, J. Electrochem. Soc. 129 (1982) 474-480.

[24] B.D. Cahan, C.T. Chen, J. Electrochem. Soc. 129 (1982) 921-925.

[25] J.R. Macdonald, J. Schoonman, A.P. Lehnen, J. Electroanal. Chem. 131 (1982) 77-95.

[26] B.E. Conway, in: E. Barsoukov and J.R. Macdonald, (Eds.), Impedance Spectroscopy (Theory, Experiment and Applications), 2nd ed., Wiley Interscience, New Jersey, 2005, pp. 469-497.

[27] T. Pajkossy, Solid State Ionics 176 (2005) 1997-2003.

[28] J.C.K. Ho, D.L. Piron, J. Appl. Electrochem. 26 (1996) 515-521.

[29] J.O'M. Bockris, T. Otagawa, J. Phys. Chem. 87 (1983) 2960-2971.

[30] J. McBreen, in: J.O. Besenhard, (Ed.), Handbook of Battery Materials, Wiley-VCH, Weinheim, 1999, pp. 135-152.

[32] L.D. Burke, M.E.G. Lyons, J. Electroanal. Chem.198 (1986) 347-368.

Figure Captions

Fig. 1 - Schematic of the expected impedance responses in the Bode format (log|Z| vs. log frequency and phase angle vs. log freq.) for an oxide covered electrode during active oxygen evolution. Several possible scenarios (1 – 4) are considered.

Fig. 2 – Electrical equivalent circuit models that may be applicable in aiding the interpretation of the experimental EIS data presented in this article.

Fig. 3 – Bode plots of EIS data recorded at various potentials for a fresh Fe electrode in 1.0 M NaOH solution. The raw data is represented by the discrete points, while the continuous lines plot the optimised transfer functions generated by CNLS fitting to Circuit A of Fig. 2. Inset – DC OER steady state polarisation plot for the same system – see ref. [20] for more details.

Fig. 4 – Bode plots recorded during oxygen evolution for an “aged” Fe electrode in 1.0 M NaOH solution. The raw data are depicted as discrete points while the continuous lines are the results of CNLS fits to Circuit A. Inset – The dc OER steady state polarisation characteristic for the same system – see ref. [19] for more details.

Fig. 5 – Bode plots of impedance data recorded at various potentials for an oxidised Co electrode in 1.0 M NaOH solution. The raw data is represented by the discrete points, while the continuous lines plot the optimised transfer functions generated by CNLS fitting to Circuit A of Fig. 2. Inset – The dc OER steady state polarisation curve for the same system – see ref. [20] for more details.

Fig.6 – Bode plots of impedance data recorded at various potentials for an oxidised Ni electrode in 1.0 M NaOH solution. The raw data is represented by the discrete points, while the continuous lines plot the optimised transfer functions generated by CNLS fitting to Circuit A of Fig. 2. Inset – The dc OER steady state polarisation characteristic for the same system – see ref. [20] for more details.

Fig. 7 – Bode representation of EIS data recorded in 1.0 M NaOH for a more aged oxidised Ni anode than that characterised in Fig. 6. Inset – The dc OER steady state polarisation plot for this aged Ni electrode in 1.0 M NaOH.

Figure 1

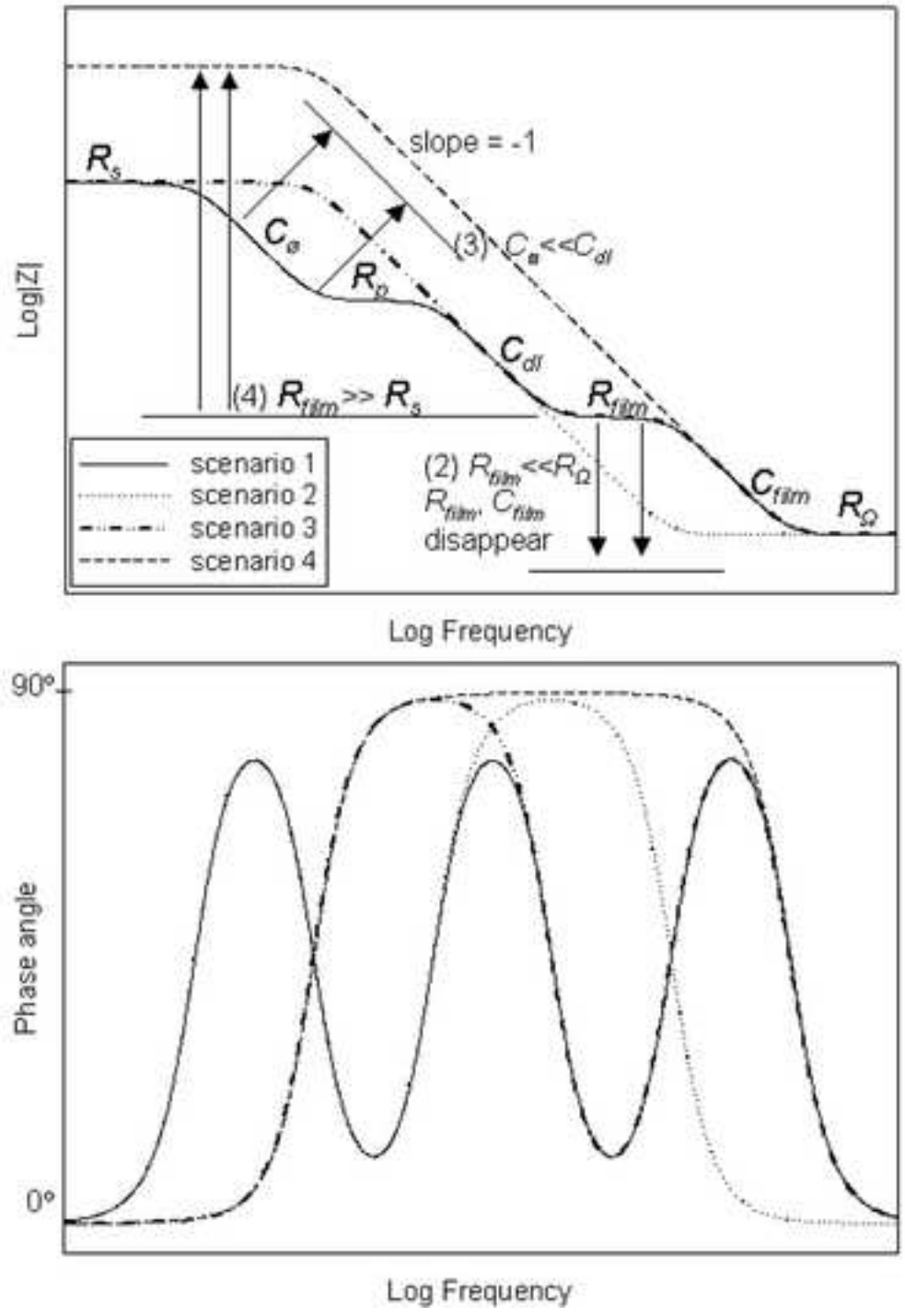
Log|Z|
slope = -1
R_s
C_a
R_Ω
(3) C_a<<C_{dl}
C_{dl}
(4) R_{film} >> R_s
R_{film}
C_{film}
R_Ω
(2) R_{film}<<R_Ω
R_{film}, C_{film}
disappear
scenario 1
scenario 2
scenario 3
scenario 4
Log Frequency
90°
0°
Phase angle
Log Frequency

Figure 2

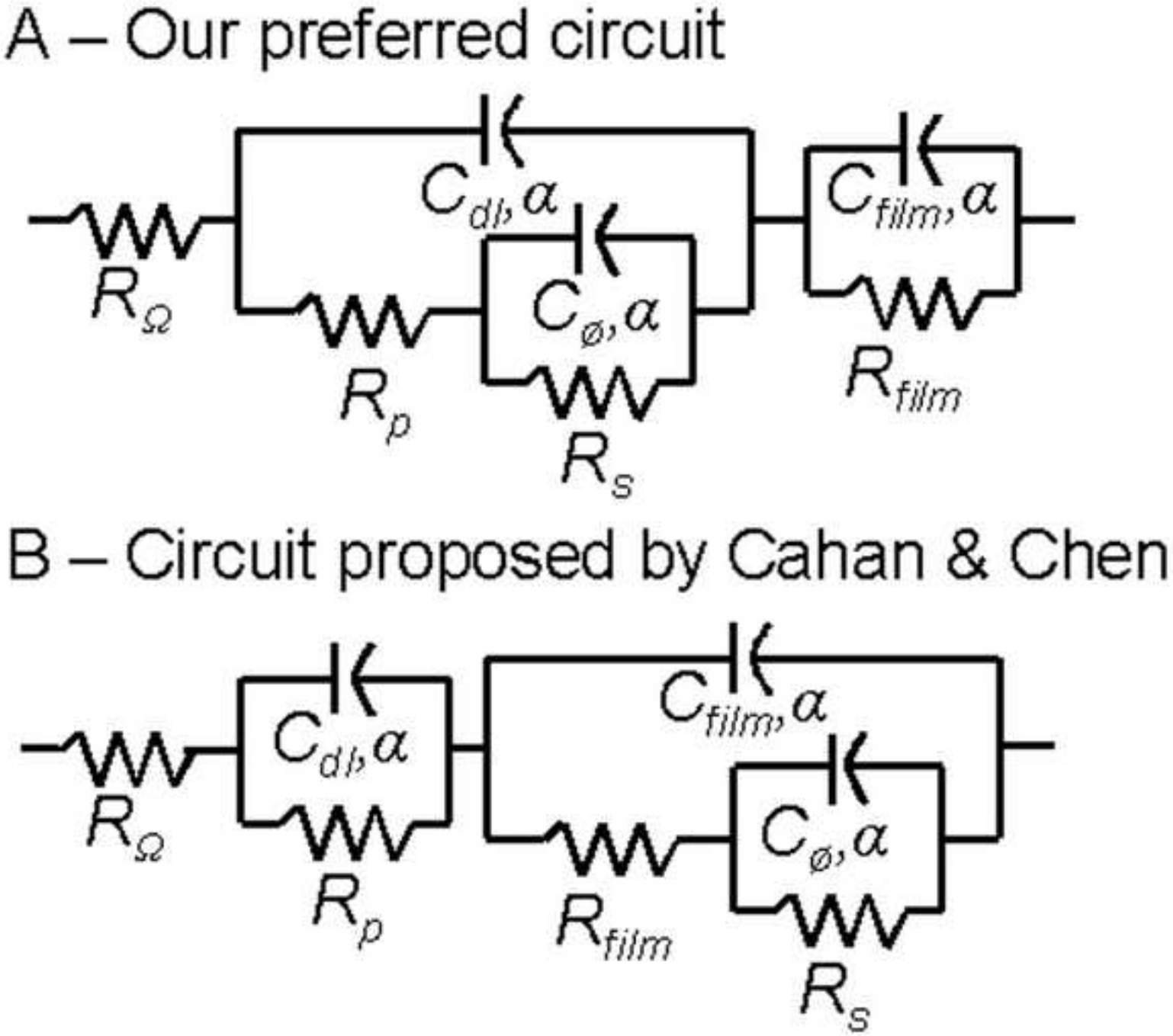
A – Our preferred circuit
C_{dl}, α
C_{film}, α
R_Ω
C_ϕ, α
R_p
R_{film}
R_s
B – Circuit proposed by Cahan & Chen
C_{film}, α
C_{dl}, α
R_Ω
C_ϕ, α
R_p
R_{film}
R_s

Figure 3

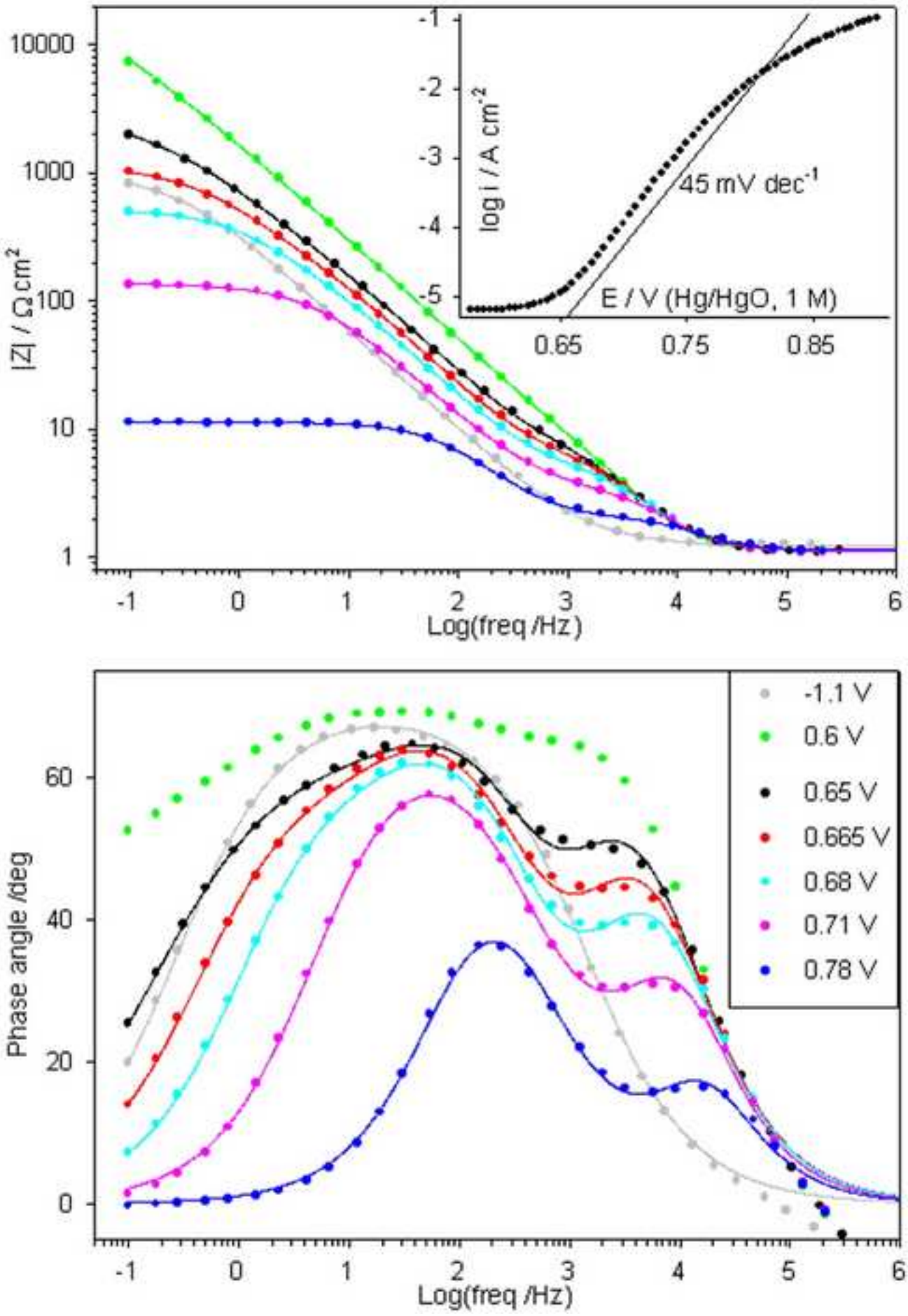

Figure 4

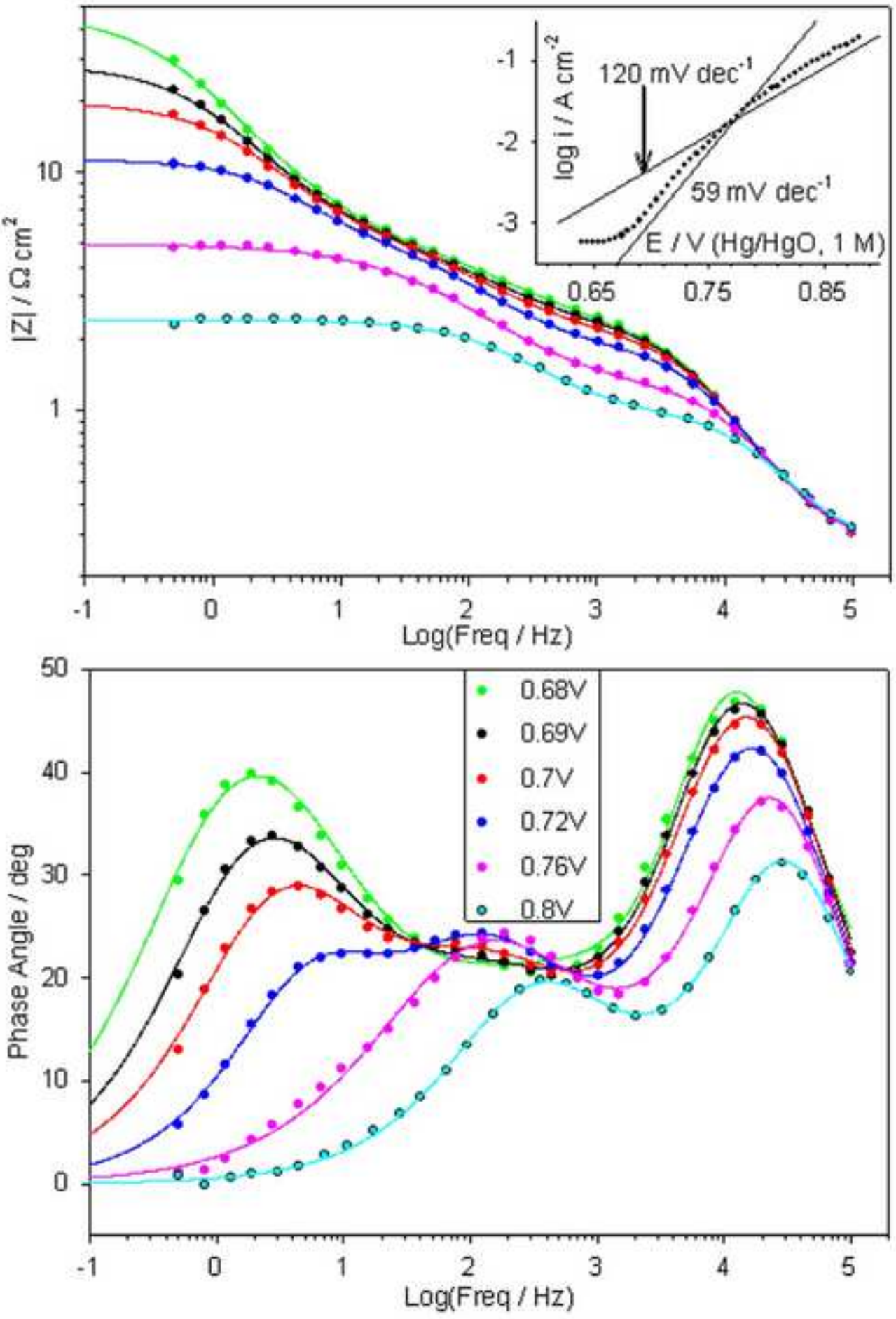

Figure 5

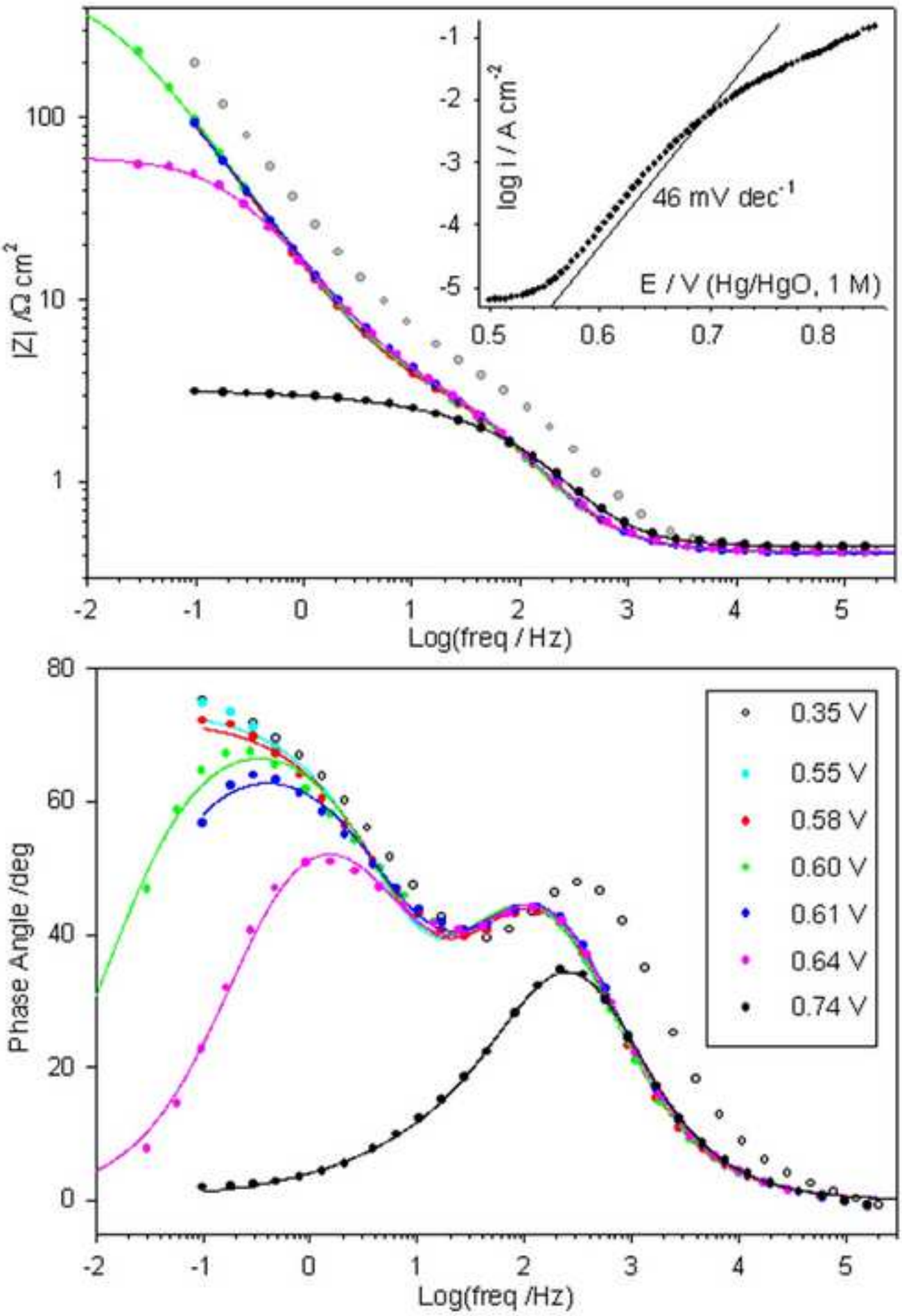

Figure 6

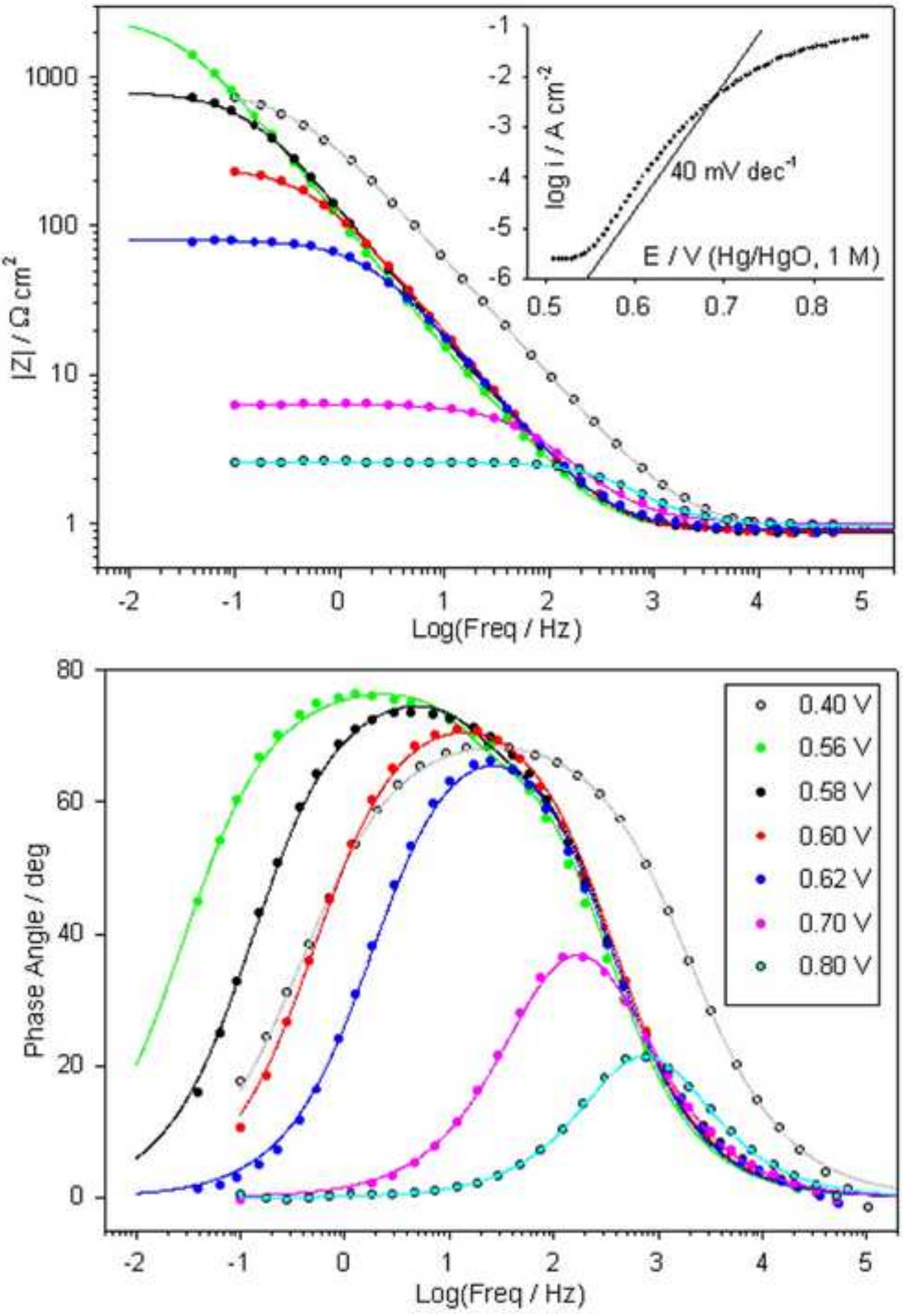

Figure 7

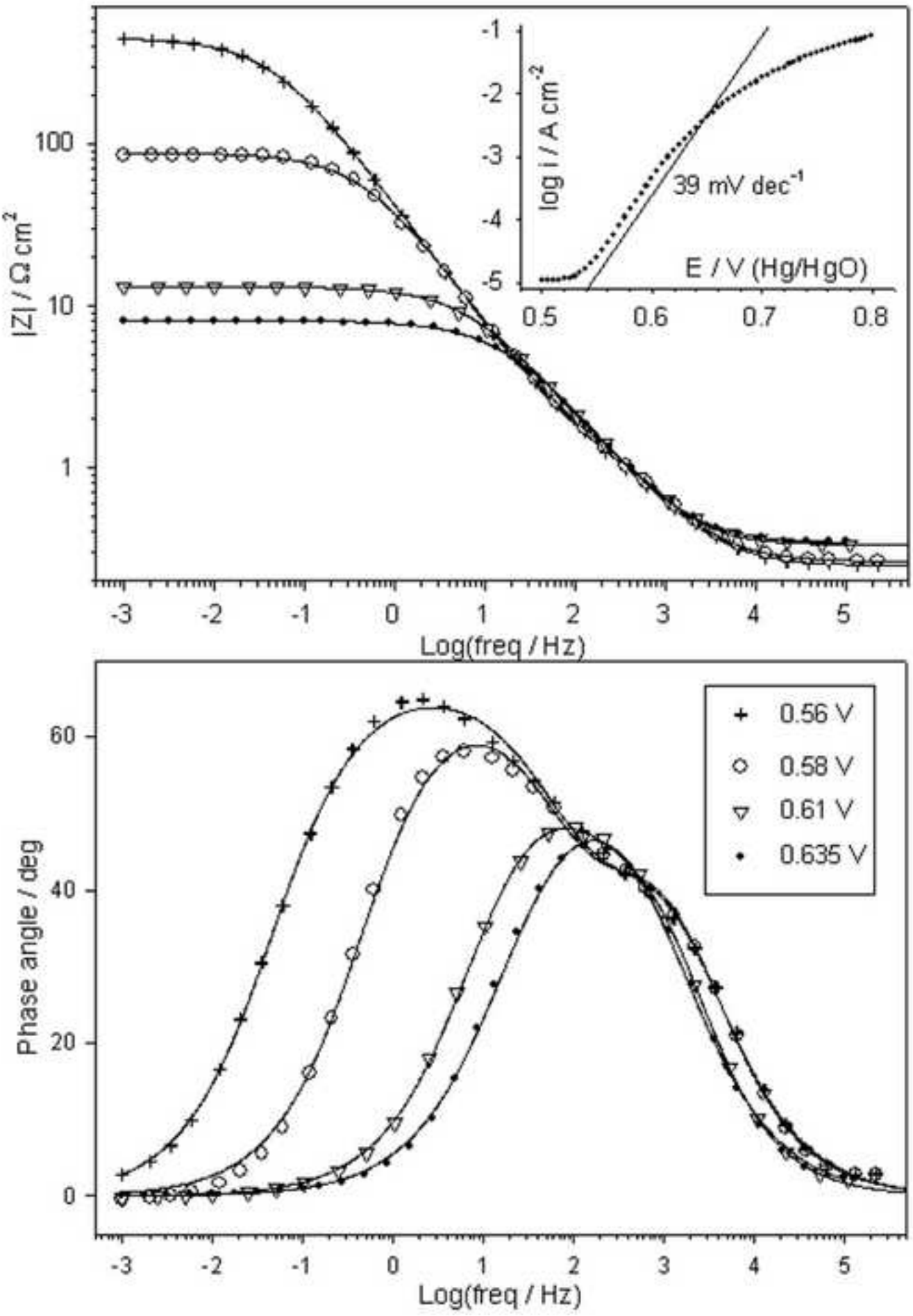

Scenario	Relative magnitude of elements	Measurable elements	Significance of R_{lf}	Comments
1	$R_s >> R_p >> R_{film} >> R_\Omega$ $C_\phi >> C_{dl} >> C_{film}$	all	$R_{lf} \approx R_{far}$	Most general situation – unlikely to be observed experimentally
2	$R_s >> R_p >> R_\Omega >> R_{film}$ Otherwise as for 1	all except R_{film} & C_{film}	$R_{lf} \approx R_{far}$	Occurs when resistance of oxide film is negligible compared with solution resistance
3	$C_{dl} >> C_\phi$ Otherwise as for 1	all except R_s & C_ϕ	$R_{lf} \approx R_{far}$	Occurs where the rate of change of fractional coverage of OER intermediate vs. potential is small
4	$R_{film} >> R_s >> R_p >> R_\Omega$ Otherwise as for 1	only R_{film}, C_{film} & R_Ω	$R_{lf} \approx R_{film}$	Arises due to poorly conductive oxide film

Table 1 – An overview of the four scenarios depicted graphically in Fig. 1.

	E V	R_s Ωcm^2	$C_{ø}(\alpha=1)$ $\mu F\ cm^{-2}$	α	R_p Ωcm^2	$C_{dl}(\alpha=1)$ $\mu F\ cm^{-2}$	α	R_{film} Ωcm^2	$C_{film}(\alpha=1)$ $\mu F cm^{-2}$	α	R_{Ω} Ωcm^2
fresh Fe	0.71	73(1.7)	49(4.1)	0.81(0.50)	59(2.0)	87(1.9)	0.85(0.35)	1.9(6.5)	20(10.1)	0.94(1.2)	1.11(6.0)
aged Fe	0.72	5.5(4.2)	2.4(6.9)	0.82(0.58)	4.3(3.6)	309(2.9)	0.74(0.43)	1.41(0.98)	22.1(2.9)	0.90(0.26)	0.27(3.4)

Table 2 – Comparison of the optimised values of the elements of Circuit A, for the fresh iron electrode data at 0.71 V and the aged iron anode data at 0.72 V. Included in parenthesis are the percentage errors in these values, calculated by the fitting program, for the frequency at which each element has its greatest significance.